



## Comparison of a Drug-Free Early Programmed Dismantling PDLLA Bioresorbable Scaffold and a Metallic Stent in a Porcine Coronary Artery Model at 3-Year Follow-Up

Kazuyuki Yahagi, Yi Yang, Sho Torii, Johanne Mensah, Roseann M White, Marion Mathieu, Erica Pacheco, Masataka Nakano, Abdul Barakat, Tahmer Sharkawi, et al.

### ► To cite this version:

Kazuyuki Yahagi, Yi Yang, Sho Torii, Johanne Mensah, Roseann M White, et al.. Comparison of a Drug-Free Early Programmed Dismantling PDLLA Bioresorbable Scaffold and a Metallic Stent in a Porcine Coronary Artery Model at 3-Year Follow-Up. *Journal of the American Heart Association*, 2017, 6 (6), 10.1161/JAHA.117.005693 . hal-01928659

**HAL Id: hal-01928659**

**<https://hal.umontpellier.fr/hal-01928659>**

Submitted on 20 Nov 2018

**HAL** is a multi-disciplinary open access archive for the deposit and dissemination of scientific research documents, whether they are published or not. The documents may come from teaching and research institutions in France or abroad, or from public or private research centers.

L'archive ouverte pluridisciplinaire **HAL**, est destinée au dépôt et à la diffusion de documents scientifiques de niveau recherche, publiés ou non, émanant des établissements d'enseignement et de recherche français ou étrangers, des laboratoires publics ou privés.

# Comparison of a Drug-Free Early Programmed Dismantling PDLLA Bioresorbable Scaffold and a Metallic Stent in a Porcine Coronary Artery Model at 3-Year Follow-Up

Kazuyuki Yahagi, MD;\* Yi Yang, MD;\* Sho Torii, MD; Johanne Mensah, MS; Roseann M. White, MA; Marion Mathieu, MS; Erica Pacheco, MS; Masataka Nakano, MD; Abdul Barakat, PhD; Tahmer Sharkawi, PhD; Michel Vert, PhD; Michael Joner, MD; Aloke V. Finn, MD; Renu Virmani, MD; Antoine Lafont, MD, PhD

**Background**—Arterial Remodeling Technologies bioresorbable scaffold (ART-BRS), composed of L- and D-lactyl units without drug, has shown its safety in a porcine coronary model at 6 months. However, long-term performance remains unknown. The aim of this study was to evaluate the ART-BRS compared to a bare metal stent (BMS) in a healthy porcine coronary model for up to 3 years.

**Methods and Results**—Eighty-two ART-BRS and 66 BMS were implanted in 64 Yucatan swine, and animals were euthanatized at intervals of 1, 3, 6, 9, 12, 18, 24, and 36 months to determine the vascular response using quantitative coronary angiography, optical coherence tomography, light and scanning electron microscopy, and molecular weight analysis. Lumen enlargement was observed in ART-BRS as early as 3 months, which progressively increased up to 18 months, whereas BMS showed no significant difference over time. Percentage area stenosis by optical coherence tomography was greater in ART-BRS than in BMS at 1 and 3 months, but this relationship reversed beyond 3 months. Inflammation peaked at 6 months and thereafter continued to decrease up to 36 months. Complete re-endothelialization was observed at 1 month following implantation in both ART-BRS and BMS. Scaffold dismantling started at 3 months, which allowed early vessel enlargement, and bioresorption was complete by 24 months.

**Conclusions**—ART-BRS has the unique quality of early programmed dismantling accompanied by vessel lumen enlargement with mild to moderate inflammation. The main distinguishing feature of the ART-BRS from other scaffolds made from poly-L-lactic acid may result in early and long-term vascular restoration. (*J Am Heart Assoc.* 2017;6:e005693. DOI: 10.1161/JAHA.117.005693.)

**Key Words:** biodegradable polymer • bioresorbable scaffold • luminal gain • optical coherence tomography • pathology • resorption • stent

Bioresorbable scaffolds (BRS) have been emerged as an alternative to metallic stents for the percutaneous treatment of obstructive atherosclerotic coronary lesions.<sup>1,2</sup> In the 1-year result of the ABSORB III randomized clinical trial, everolimus-eluting bioresorbable vascular scaffold (Absorb BVS, Abbott Vascular, Santa Clara, CA) showed noninferiority for target lesion failure compared with the everolimus-eluting Xience drug-eluting stent (Abbott Vascular, Santa Clara, CA).<sup>3</sup>

However, a recent ABSORB II trial did not meet its primary end point of superior vasomotor reactivity and larger late lumen loss in Absorb BVS at 3 years after implantation, compared with the Xience drug-eluting stent.<sup>4</sup> In addition, the Absorb BVS showed a significantly higher device-oriented composite end point with higher incidence of scaffold thrombosis.<sup>5</sup> Many BRSs have been investigated in preclinical studies,<sup>6,7</sup> where degradation kinetics have been variable.

From the CVPATH Institute, Gaithersburg, MD (K.Y., S.T., E.P., M.N., M.J., A.V.F., R.V.); Université Paris-Descartes, Paris, France (Y.Y., A.L.); Cardiology Department, European Georges Pompidou Hospital, APHP, Paris, France (Y.Y., A.L.); PARCC, INSERM U970, Paris, France (Y.Y., A.L.); Hydrodynamics Laboratory (LadHyX), CNRS UMR7646, Ecole Polytechnique, Palaiseau, France (J.M., A.L., A.B.); Pragmatic Clinical Trial Statistics, Durham, NC (R.M.W.); Arterial Remodeling Technologies, Paris, France (M.M.); Faculty of Pharmacy, Institut des Biomolécules Max Mousseron, UMR CNRS 5247, University Montpellier 1-CNRS, Montpellier, France (T.S., M.V.).

\*Dr Yahagi and Dr Yang contributed equally to this work.

**Correspondence to:** Antoine Lafont, MD, PhD, Cardiology Department, Hôpital Européen Georges Pompidou, 20 rue Leblanc, 75908 Paris, France. E-mail: antoine.lafont@inserm.fr

Received February 7, 2017; accepted April 19, 2017.

© 2017 The Authors and Arterial Remodeling Technologies. Published on behalf of the American Heart Association, Inc., by Wiley. This is an open access article under the terms of the Creative Commons Attribution-NonCommercial License, which permits use, distribution and reproduction in any medium, provided the original work is properly cited and is not used for commercial purposes.

## Clinical Perspective

### What Is New?

- The ART-BRS is made of 98% L-lactic acid and 2% D-lactic acid, designed to degrade starting at 3 months with complete polymer resorption at 2 years. Because of the above characteristics, we observed early positive remodeling beginning from 3 to 6 months with a peak at 18 months associated with lumen enlargement, without severe inflammation. The lumen area from 18 to 36 months remained the same size without any vessel shrinkage.

### What Are the Clinical Implications?

- Early endothelial coverage of BRS without drug may allow early discontinuation of the dual antiplatelet therapy. The early dismantling results in early lumen recovery. This early degradation of ART-BRS is less likely to lead to late scaffold thrombosis.

From these preclinical studies, it is clear that slow degradation of polymeric BRS was considered safe and was associated with mild inflammation.<sup>6,7</sup> However, a more rapid onset of degradation may facilitate early vessel remodeling and luminal gain during the course of vascular healing and consequently may decrease detrimental vascular effects that have recently been reported over the long term in man.<sup>3,4</sup>

We investigated the Arterial Remodeling Technologies (ART, Paris, France) BRS, composed of L- and D-lactyl units instead of only L-lactyl units with the distinguishing feature of early programmed dismantling. The dismantling of ART-BRS began at 3 months after implantation, which allowed for rapid vascular restoration with progressive lumen enlargement up to 6 months.<sup>2,8,9</sup> The aim of the current study was to characterize the vascular response following implantation of a novel ART-BRS in comparison to bare metal stents (BMS) by angiography, histopathology, and biochemical analysis of molecular weight up to 36 months in a healthy porcine coronary artery model.

## Methods

### Study Design and Animal Experiments

The ART-BRS is made of polylactic acid (PLA) 98, a stereocopolymer composed of 98% L-lactic acid and 2% D-lactic acid with strut thickness of 170  $\mu\text{m}$  without a drug, and has a design that is flexible, resulting in a stent-to-luminal-surface ratio of <25%. The study protocol was reviewed, approved by an Institutional Animal Care and Use Committee, and performed at AccellLAB (Montreal, Canada); it was conducted in accordance with the Canadian Council on Animal Care regulations.

ART-BRS (Arterial Remodeling Technologies, Paris, France) 3.0×11 mm and control BMS (Multilink Vision, Abbott, Santa Clara, CA) 3.0×12 mm were randomly implanted into the major coronary arteries and had a stent/scaffold-to-artery ratio of  $\approx 1.1$  to 1.2:1.0 in the coronary arteries of healthy Yucatan female or castrated male miniswine (30–50 weeks, Lone Star Laboratory Swine, Sioux Center, IA) via femoral access following standard procedures as previously described.<sup>9</sup> All but 4 animals received an ART-BRS and a BMS (36 animals received 1 ART-BRS and 1 BMS implant in 2 separate arteries, 17 animals received 2 ART-BRS and a single BMS in 3 separate arteries, and 7 animals received 1 ART-BRS and 2 BMS in 3 separate arteries). The other 4 animals received 2 ART-BRS in 2 separate arteries but no BMS for chemical analysis/molecular weight (total ART-BRS 82, BMS 68). Sixty-four animals were further divided into various cohorts depending on the duration of implantation; 1 month (n=10), 3 months (n=11), 6 months (n=9), 9 months (n=7), 12 months (n=8), 18 months (n=7), 24 months (n=6), and 36 months (n=6) (Table). Quantitative coronary angiography (QCA) was performed in all animals before they were euthanatized. Optical coherence tomography (OCT) was performed in 3 ART-BRS and 3 BMS at each time point.

### Quantitative Coronary Angiography

QCA was carried out and analyzed by an independent core laboratory (AccellLAB, Montreal, QC, Canada) as previously described.<sup>9</sup> The Medis QCA-CMS 6.0 system (Raleigh, NC) was used for QCA measurement. The following parameters were included in this study: mean lumen diameter at preimplantation, balloon-to-artery ratio, minimal lumen diameter (MLD) at postimplantation and follow-up, diameter stenosis, and late lumen loss. Acute gain was calculated as MLD at postimplantation minus mean lumen diameter at preimplantation. Diameter stenosis was calculated as 1–MLD/reference vessel diameter at explant. Late lumen loss was calculated as MLD at postimplantation minus MLD at follow-up.

### Optical Coherence Tomography

OCT was performed with a commercially available C7 OCT system (St Jude Medical, St Paul, MN). Quantitative analysis was performed with ILUMIEN software (LightLab Imaging, Westford, MA), with 5 sections coregistered with histology. Quantitative area measurements included inner stent/scaffold area and lumen area as previously described.<sup>10</sup> Neointimal thickness was calculated as (inner stent or scaffold diameter–lumen diameter)/2. The percentage stenosis relative to the reference vessel segment was defined as 1–(minimum lumen area within the stented or scaffolded

**Table.** Summary of Studied Animals and Implanted Materials for Light Microscopy, Scanning Electron Microscopy, and Gel Permeation Chromatography

	1 Month	3 Month	6 Month	9 Month	12 Month	18 Month	24 Month	36 Month	Total
Total pigs	10	11	9	7*	8	7	6*	6*	64 (61)*
Light microscopy implants									
ART-BRS	8	7	8	10 (8)*	8	8	7 (6)*	8 (7)*	64 (60)*
BMS	8	8	8	9 (8)*	7	8	8 (6)*	8 (6)*	64 (59)*
SEM implants									
ART-BRS	2	2	0	0	0	0	0	0	4
BMS	2	2	0	0	0	0	0	0	4
GPC implants									
ART-BRS	2	2	2	2	2	2	2	0	14
Total ART-BRS+BMS, analyzed	22	21	18	18	17	18	14	13	141

Coronary angiography was performed in all implanted animals that completed the in-life part of the study. ART-BRS indicates Arterial Remodeling Technologies bioresorbable scaffold; BMS, bare metal stent; GPC, gel permeation chromatography; SEM, standard error of the mean.

\*Three animals died with 4 ART-BRS and 5 BMS implants, and the parentheses show the actual number examined by light microscopy in the groups where animals died.

segment)/reference lumen area. BRS strut images were classified by morphology and signal intensity into 4 categories as previously described,<sup>11</sup> and the percentage in each category was determined.

## Histological Assessment

Hearts were pressure-perfusion fixed in 10% neutral buffered formalin at 80 to 100 mm Hg. The implanted coronary arteries were dissected from the heart and radiographed before embedding in glycol methacrylate for ART-BRS and methylmethacrylate for BMS. After polymerization, histologic sections were prepared at 4- to 6- $\mu$ m thickness from the proximal, middle, and distal regions of each device and stained with hematoxylin and eosin and Miller elastic stain. Proximal and distal nonstented segments were prepared for paraffin histology at 4- to 6- $\mu$ m thickness and stained with hematoxylin and eosin and Movat pentachrome. All histologic sections were examined for inflammation, fibrin, giant cell reaction, and vessel injury as previously described.<sup>12</sup> Strut discontinuities were defined as sites that showed deviation from the conventional box shape with integration of arterial derived tissue on a cross-sectional level.<sup>7</sup> Strut resorption sites were identified by the presence of a glassy appearance, with either eosinophilic or amphophilic staining by hematoxylin and eosin and under polarized light.<sup>7</sup> Histomorphometry was performed using computer-assisted software (IPLab, Scanalytics, Rockville, MD) as previously described.<sup>13</sup>

## Scanning Electron Microscopy

Scanning electron microscopy was performed to examine the extent and maturation of surface re-endothelialization of

implanted devices. The implanted vessels were bisected longitudinally and photographed. Specimens were postfixed in 1% osmium tetroxide, dehydrated in graded series of ethanol solutions, critical-point dried, and sputter-coated with gold as previously described.<sup>14</sup> All specimens were visualized using a Hitachi 3600N scanning electron microscope.

## Chemical Analysis of Molecular Weight

The in vivo average polymer molecular weight was quantified using size exclusion chromatography at all time points as previously described.<sup>9</sup> The monitoring of in vitro hydrolytic degradation was carried out in parallel. ART-BRS were allowed to age at 37°C in vials in the presence of sterile isosmolar (0.13 mol/L) pH=7.4 phosphate buffer.

## Statistical Analysis

Continuous values with normal distribution were expressed as mean $\pm$ standard deviation. Normality of distribution was checked using graphical methods and the Shapiro-Wilk test. Variables with nonnormal distribution were expressed as median with 25th and 75th percentiles. A linear mixed model was used to compare the stent to the scaffold over time. Treatment (scaffold versus stent) time point and their interaction were considered fixed effects. Given that changes over time were not linear, and the same animal was NOT tested over time, the time point was treated as an ordinal value. This maintains the ordering of the time points, but they are treated as if they are equivalent. Although the last 3 time points are farther apart than the first 4, for the purposes of testing differences the profiles between the 2 treatment groups, treating each time point equally does not detract from



the generalizability of the results. The animal was specified as a random effect to account for the effects individual animals might have on the outcomes. Dependent variables with nonnormal distribution were logarithmically transformed before the analyses. A value of  $P < 0.05$  was considered statistically significant. SPSS software (version 22.0, Chicago, IL) and JMP software (version 5.0 and version 13.1, Cary, NC) were used for statistical analyses.

## Results

Three animals were euthanatized before the scheduled explant time. The first animal in the 9-month cohort implanted with 2 ART-BRS and 1 BMS and the second animal in the 24-month cohort implanted with 1 ART-BRS and 2 BMS were euthanatized before the scheduled explant time (at 149 and 133 days, respectively). One animal in the 9-month cohort had a reduced appetite, and despite vitamin treatment, the animal's condition showed no improvement (no other abnormality was found either in veterinary observation or blood

parameters). An animal in the 24-month cohort had a reduced appetite and suffered from otitis. Despite antibiotic treatment, the animal's condition showed no improvement. Mild neointimal growth and inflammation were observed in the stented coronary segments. The third animal in the 36-month cohort implanted with 1 ART-BRS and 2 BMS died during the 6-month control angiography from ventricular fibrillation. This kind of complication is not unusual, especially when high volumes of contrast media are injected for OCT. The BRS and BMS were both open and showed there were granulomas around the BRS; however, the BMS was without any inflammation (Figure 1). All other animals completed the in-life phase of the study.

## Quantitative Coronary Angiography Analysis

Relatively acute recoil was lower in ART-BRS than in BMS but did not reach significance between the 2 groups ( $P = 0.146$ , Figure 2). The balloon-to-artery ratio was higher over time for BMS than for ART-BRS ( $P = 0.008$ ), but the profiles were not

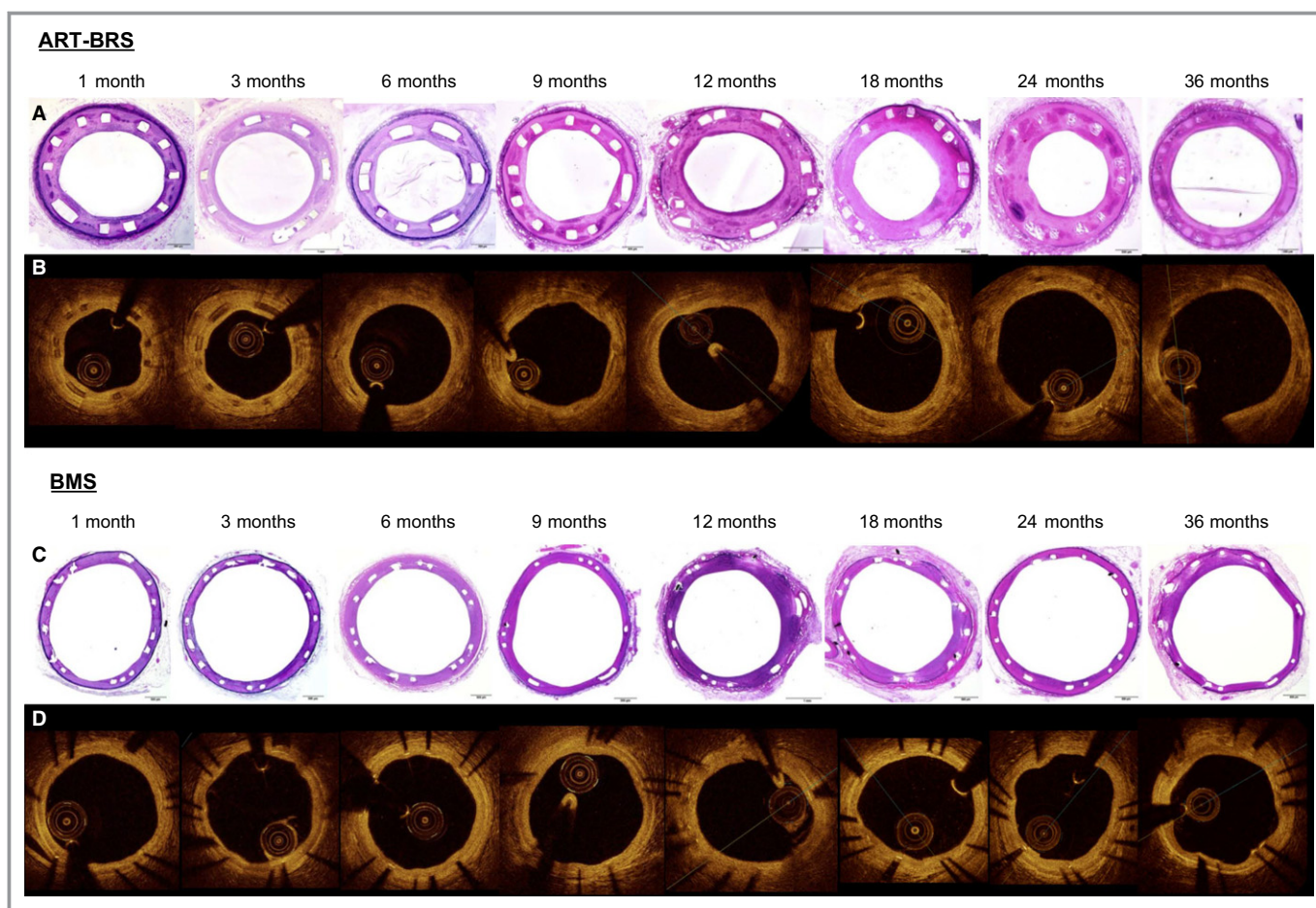


**Figure 1.** Representative histology of Arterial Remodeling Technologies bioresorbable scaffold (ART-BRS) (A) and bare metal stent (BMS) (C) with coregistered images of optical coherence tomography (ART-BRS, B; BMS, D) in a porcine coronary artery model from 1 to 36 months.

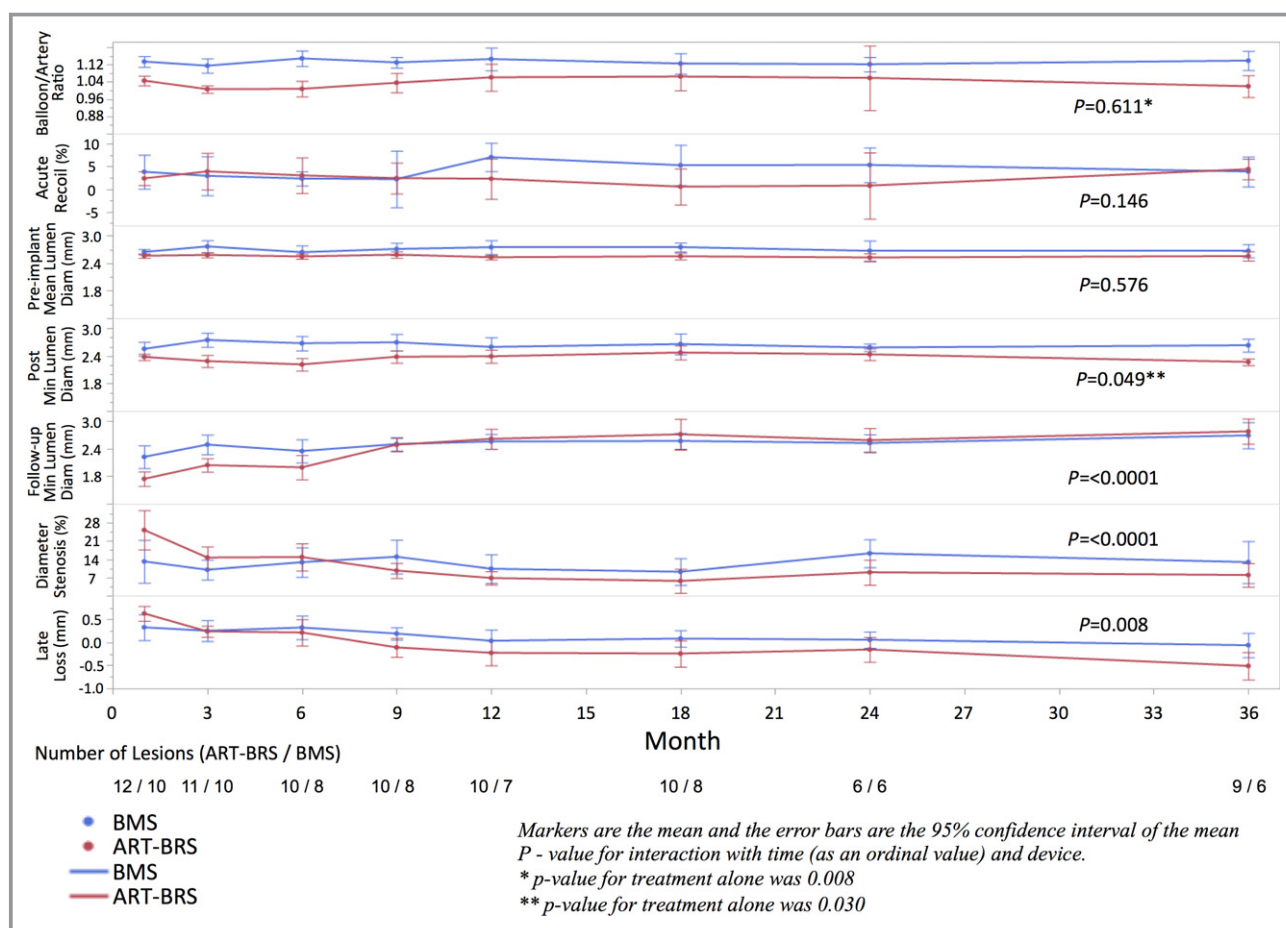


**Figure 2.** Summary of the results of the quantitative coronary angiography analysis. Each plot shows the mean and 95% confidence interval for each treatment over time for balloon/artery ratio, percentage acute recoil, preimplant mean lumen diameter, postprocedure minimum lumen diameter, follow-up minimum lumen diameter, percentage diameter stenosis, and late loss.

statistically different over time ( $P=0.611$ ). The preimplant mean lumen diameter ratio was observed to be higher over time for BMS than for ART-BRS, but the difference did not achieve statistical significance. The postprocedure minimum lumen diameter was higher over time for the BMS than the ARTS-BRS ( $P=0.03$ ) (as expected because the preprocedure mean diameter was higher), and the profile showed over time was significant ( $P=0.049$ ) due to the responses at 3 and 6 months. A similar pattern was observed in the mean lumen diameter, but it did not achieve statistical significance. The results from these measures indicate consistency in the application of the implantation procedure for each type of implant. There was a significant difference in percentage diameter stenosis over time between the 2 stents ( $P<0.0001$ ): stenosis with the ART-BRS was greater than that with the BMS at 1 month ( $25.3\pm 11.9\%$  versus  $13.2\pm 11.5\%$ , respectively) and 6 months ( $14.9\pm 7.4\%$  versus  $12.9\pm 6.8\%$ , respectively) but less than that with the BMS from 9 to 36 months (Figure 2). Similarly, there was a significant difference in late lumen loss over time between the 2 stents ( $P=0.0008$ ). The

late loss was higher with the ART-BRS than with the BMS at 1 month ( $0.64\pm 0.26$  mm versus  $0.33\pm 0.40$  mm, respectively). At 9 months, however, late lumen loss reversed to late lumen gain (negative late lumen loss) in ART-BRS. This trend was further augmented at 12, 24, and 36 months, with late lumen gain reaching 0.22, 0.15, and 0.51 mm, respectively.

## Quantitative OCT Analysis

The representative OCT images of ART-BRS and BMS coregistered with histology are shown in Figure 1. Lumen enlargement was observed in ART-BRS as early as 3 months following implantation, and it progressively increased and peaked at 18 months ( $8.9$  mm<sup>2</sup>), paralleling the dynamic increase of scaffold area over time, whereas BMS showed no significant difference in lumen area or stent area over time ( $\approx 5.8$  mm<sup>2</sup>) (Figure 3A). Percentage stenosis relative to the reference vessel segment decreased over time in ART-BRS and was less than 10% after 18 months, whereas in BMS, it increased up to  $\approx 40\%$  after 9 months and remained stable up to 36 months.

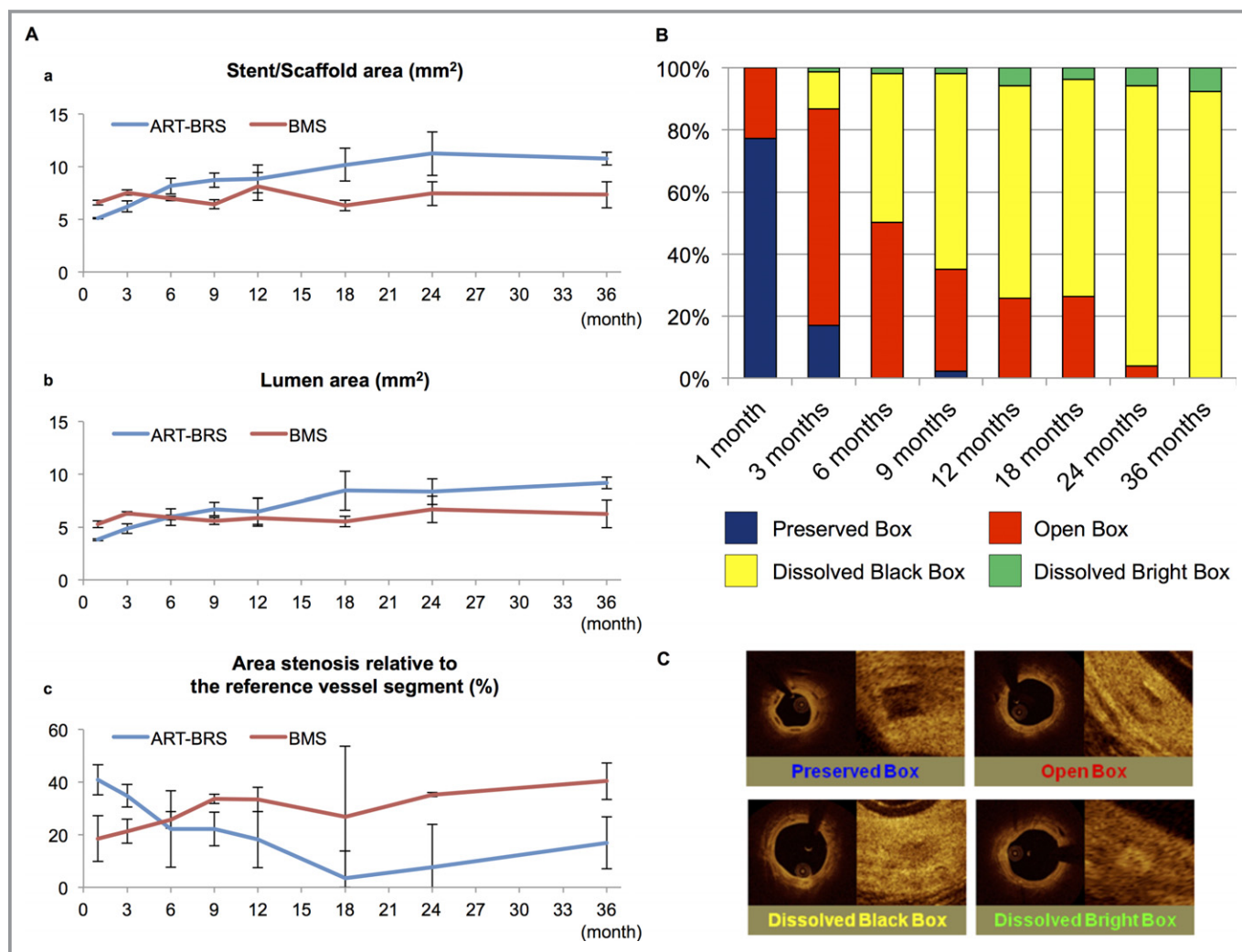


**Figure 3.** Measurement of optical coherence tomography (OCT) (A) and strut classification (%) (B) of Arterial Remodeling Technologies bioresorbable scaffold (ART-BRS) and bare metal stent (BMS). Line graphs show stent/scaffold area (a), lumen area (b), and area stenosis relative to the reference vessel segment (c) by optical coherence tomography analysis. The blue line represents BRS, and the red line represents BMS. Data are presented as mean±standard deviation. C, Representative images of strut classification by optical coherence tomography.

## Qualitative OCT Analysis

Scaffold strut classification of ART-BRS and representative strut appearances of each category observed by OCT are shown in Figure 3B and 3C. The percentage of preserved boxes rapidly decreased in the first 3 months (77% at 1 month and 17% at 3 months), and only very few were detected from 6 to 24 months. The percentage of open boxes showed a peak at 3 months, followed by a progressive decrease, and remained at 4% at 24 months. The proportion of dissolved black boxes increased to 66% at 9 months, and a majority of struts showed dissolved black boxes at 24 and 36 months (90% and 92%, respectively), whereas dissolved white boxes were maximum at 36 months (8%).

## Histology Analysis

All ART-BRS struts were well opposed to the artery wall, with complete endothelialization at all time points (Figure 4A). There was an absence of thrombus formation for both ART-BRS and BMS at all time points. All struts were completely incorporated within neointimal growth.

Observed mean injury scores were higher in ART-BRS compared with BMS at all time points, but they did not reach statistical significance ( $P=0.089$ , Figure 4B). Inflammatory score peaked at 6 months (1.83 [IQR 1.08-2.85]) and thereafter continued to decrease up to 36 months (0.60 [IQR 0.33-1.00]) in ART-BRS. As expected, the inflammatory scores were higher in ART-BRS than in BMS but did not reach statistical significance ( $P=0.064$ ). Giant cell reaction around



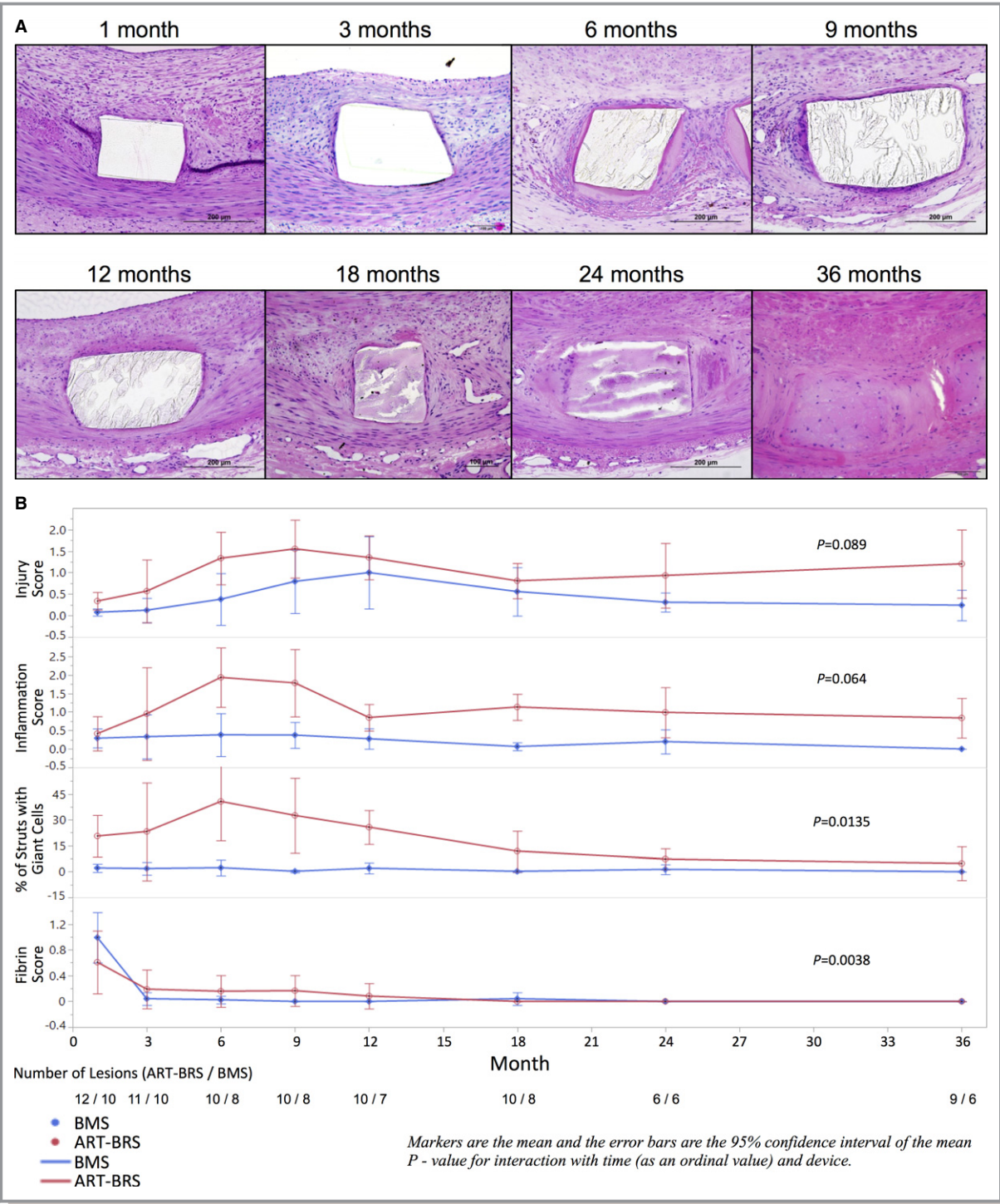


**Figure 4.** A, Representative histological images of Arterial Remodeling Technologies bioresorbable scaffold (ART-BRS) in porcine coronary arteries from 1 to 36 months. B, Results from the histology analysis. Each plot shows the mean and 95% confidence interval for each treatment over time for injury score, inflammation score, percentage of struts with giant cells, and fibrin score.

the scaffold also peaked at 6 months (38.2% [IQR 18.1-65.8]) and decreased thereafter, with significantly greater scores for ART-BRS than for BMS ( $P=0.0135$ ). As expected, fibrin deposition was minimal in both ART-BRS and BMS and was significantly different over time ( $P=0.0038$ ).

### Scanning Electron Microscopic Analysis

Scanning electron microscopy revealed uniform and complete endothelialization with endothelial cells arranged in spindle and cobblestone morphology, generally with tight junctions in



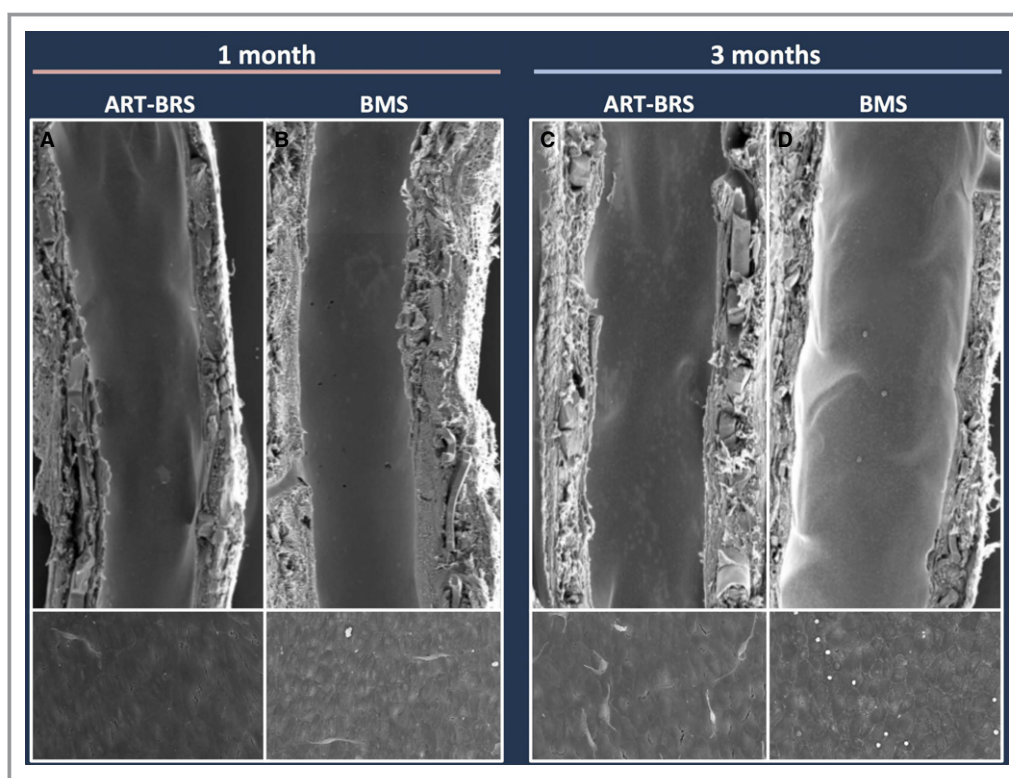


**Figure 5.** Representative scanning electron microscopy images of Arterial Remodeling Technologies bioresorbable scaffold (ART-BRS) at 1 and 3 months following implantation in porcine coronary arteries. The low-power images show complete strut coverage at 1 month in both ART-BRS (A) and bare metal stent (BMS) (B), with similar findings at 3 months (C, ART-BRS; D, BMS). High-power images also show complete endothelialization by neointima with cells arranged in spindle and cobblestone morphology and showing well-formed cell-to-cell contacts in both ART-BRS and BMS.

both devices at 1 and 3 months (Figure 5). Rarely, inflammatory cells were observed attaching to the luminal surface of both devices at 1- and 3-month follow-up.

### Chemical Analysis of Molecular Weight

By size exclusion chromatography, the molecular weight of ART-BRS struts decreased rapidly starting at 1 month, and by 3 months it had decreased to 25% of the initial value in vitro (Figure 6). The molecular weight of strut residues was very small and below the level of detection at 18 months. The in vivo decrease profile was remarkably similar to that observed under in vitro conditions.

### Intended Scaffold Dismantling and Discontinuity

Under polarized light, progressive changes could be seen in the scaffold within the first 3 months, which were characterized as layered birefringence of struts (Figure 7). Most of the scaffolds showed a mottled birefringence from 6 to 12 months, whereas only minimal birefringence was observed at 18 months, and there was a uniform absence of any birefringence after 24 and 36 months.

Histologic strut discontinuities, defined as sites in which struts deviated from the conventional box shape with integration of artery-derived tissue, were observed at 1 month onward without significant luminal compromise (Figure 7). The histologic strut discontinuities with scaffold degradation were present in 63% of struts at 12 months, becoming 100% at 18 months. Eosinophilic staining of the scaffolds (histologic scaffold degradation) was observed at 18 months and beyond, which likely represented proteoglycan infiltration of scaffold strut resorption sites (Figures 1, 4A, and 7).

### Discussion

The current study represents a comprehensive analysis of the ART-BRS using angiographic, histopathologic, and chemical degradation analysis in healthy porcine coronary arteries at multiple time points ranging from 1 to 36 months. The salient findings of this study can be summarized as follows: (1) ART-BRS showed a similar safety profile to control BMS, with complete endothelialization of struts at 1 month and absence of stent thrombosis; (2) lumen enlargement was observed from 3 months and continued to increase up to 36 months; (3) inflammatory reaction increased in ART-BRS within the

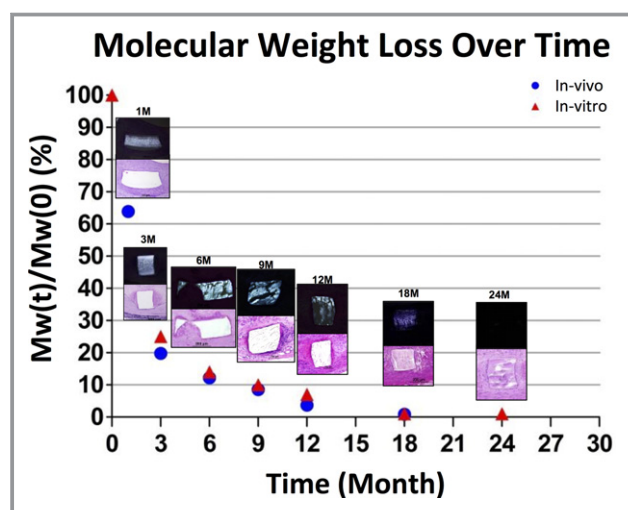


**Figure 6.** Molecular weight loss over time. Molecular weight (Mw) indicates polymer molecular weight of Arterial Remodeling Technologies bioresorbable scaffold (ART-BRS). The values are presented by the average Mw at each time point divided by the initial in vitro Mw. At 24 months, in vivo Mw was undetectable due to the ART-BRS resorption. The scaffold struts showed a glassy appearance under polarized light at 1 and 3 months. There were progressive changes, and most of the scaffolds showed a mottled appearance after 6 months, whereas minimal polarization was observed at 18 months. Eventually, uniformly, absence of any polarization was seen at 24 months.

first 6 months and decreased thereafter, with predominance of mild to moderate monocyte infiltration and giant cell reaction in the area surrounding degrading scaffold struts; and (4) a faster dismantling profile resulted in early vascular restoration of porcine coronary arteries provoking greater inflammation and luminal gain as compared with BMS.

## Lumen Gain: a Hallmark of Early BRS Degradation

We have previously reported that dismantling of the ART-BRS occurs as early as 3 months after scaffold implantation according to micro-computed tomography.<sup>9</sup> Early dismantling is the dominant feature of the ART-BRS and was confirmed by OCT imaging and histopathologic assessment. Size exclusion chromatography analysis demonstrated rapid polymer degradation of the ART-BRS, with approximately only 10% of the initial molecular weight remaining after 6 months and absence of detectable polymer residues at 24 months. The light microscopic findings of polymer breakdown as assessed by polarized light and histology also revealed progressive changes of polymer resorption sites. In the current study there was a clear agreement between chemical analysis of polymer degradation and polarized light findings by histology, which coincided with significant lumen enlargement as a function of incremental mass loss and decreasing scaffolding forces.

Early luminal enlargement initiating at 3 months following implantation was a key feature of the ART-BRS device, which is significantly faster compared with what has been reported with other bioresorbable devices made of PLLA.<sup>7,11</sup> The juvenile porcine model undergoes vessel enlargement due to the growth. However, the lumen enlargement was observed with the ART-BRS, not with BMS, which confirms the positive role of the ART-BRS. In the current study of ART-BRS, QCA analysis demonstrated greater late lumen loss compared with BMS at 1 month, resulting from early neointimal formation; however, this lumen loss was overcome by progressive luminal enlargement from 3 months onward. Inflammation was greater in ART-BRS relative to BMS and peaked at 6 months, which likely reflects maximum decrease in molecular weight and release of soluble degradation products that coincide with luminal gain as a result of vascular remodeling. It has been reported inflammation is observed from 12 to 36 months in Absorb BVS with late lumen enlargement.<sup>7</sup> The exact timing of inflammation likely varies in human disease conditions, where the early onset of inflammation in ART-BRS relative to other contemporary BRS may allow for early remodeling.

## Comparison to Contemporary Bioresorbable Scaffolds

ART-BRS is made of an L- and D-lactic acid stereocopolymer rich (98%) in L-lactyl units (PLA 98). This particular PLA-type polymer exhibits similar mechanical properties but a different resorption profile when compared with poly-L-lactic acid (PLLA; PLA 100) used in other devices such as Absorb BVS, DESolve BRS (Elixir Medical Corporation, Sunnyvale, CA) and the Igaki-Tamai scaffold.<sup>15</sup> It is well known that structures, material characteristics, and degradation processes of lactic acid-based polymers are contingent on a number of conditional factors,<sup>16,17</sup> of which the presence of a small proportion of D-lactyl units, the lower crystallinity, and the use of zinc lactate instead of stannous octoate as initiator of polymerization are likely responsible for the observed difference in dismantling rate and resorption time relative to comparative devices.<sup>18</sup>

On an angiographic level, ART-BRS exhibited augmented lumen gain when compared with the Abbott BVS: late lumen loss for ART-BRS at 12, 18, and 24 months was  $-0.22$ ,  $-0.24$ , and  $-0.15$  mm, whereas for BVS it was  $0.29$ ,  $0.02$ , and  $-0.03$  mm, respectively.<sup>7</sup>

Recent meta-analysis showed an increased risk of scaffold thrombosis for Absorb BVS at 1-year follow-up,<sup>5</sup> and this increase in stent thrombosis is also observed late at 3 years with 6 in 329 patients (2%) having very late scaffold thrombosis.<sup>4</sup> Optimized implantation strategy with OCT and longer dual antiplatelet therapy would likely reduce acute and subacute scaffold thrombosis<sup>19</sup>; however, timing of the



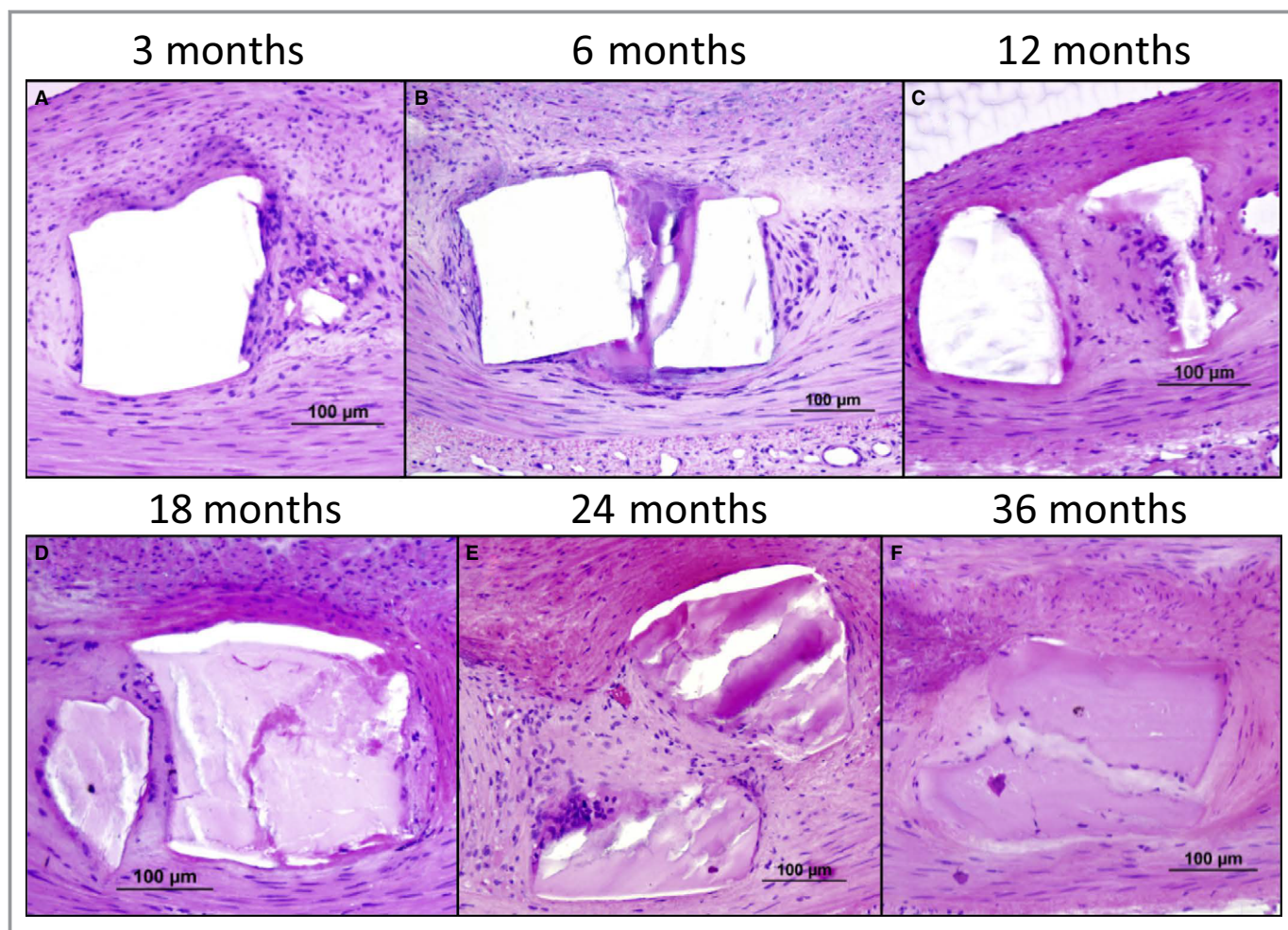


**Figure 7.** Representative images of strut discontinuities at 3 months (A), 6 months (B), 12 months (C), 18 months (D), 24 months (E), and 36 months (F).

termination of dual antiplatelet therapy is important to determine as scaffold has been shown to persist even at 5 years after implantation.<sup>20</sup> To overcome the adverse end points, second-generation bioresorbable scaffolds should be thinner and have a faster degradation profile, but radial strength must be comparable to a metallic drug-eluting stent. However, thickness of struts is likely to reduce radial strength and therefore remains a tradeoff that has not yet been achieved.

### Intravascular Imaging Findings

Intravascular imaging by OCT provides invaluable insights into the dynamic changes of vascular remodeling following the implantation of BRS.<sup>11</sup> In the current study strut degradation was assessed by OCT and characterized using previously reported terminology by Onuma et al.<sup>11</sup> For ART-BRS, preserved box appearance dominated at 1 month (77.3%) and decreased to 17.0% at 3 months, and after 9 months only a limited number of preserved boxes remained. The current

morphologic OCT analysis of scaffold struts confirmed that ART-BRS achieved a more rapid resorption than other established devices such as Absorb BVS: the corresponding values were 82% preserved box appearance at 3 months, with 79% remaining as preserved boxes at 24 months.<sup>11</sup> Preserved box appearance of BRS struts correlated with intact polymeric scaffold struts on a histological level, with neointimal tissue mainly composed of smooth muscle cells in a proteoglycan matrix.<sup>11</sup> The histological characterization of stent struts at 2-year follow-up revealed a predominance of open acellular regions with well-defined borders in the Absorb BVS,<sup>11</sup> whereas in the current study, the ART-BRS exhibited almost complete replacement of strut resorption sites by proteoglycan matrix after 18 months.

### Implications of Acute Strut Disruption and Strut Discontinuity

Acute strut disruption (within days or few weeks after implantation) of a scaffold secondary to excessive

mechanical stress during implantation in specific lesion subsets has been associated with loss of radial strength and increased thrombotic risk.<sup>21–23</sup> Furthermore, it is important to differentiate acute strut disruption from strut discontinuity resulting from intended dismantling, which is determined by a number of factors ranging from polymer composition, its degradation kinetics, and possible inflammatory reaction. Acute strut disruption is likely the result of device stiffness and excessive balloon pressure during implantation, which may lead to recoil and abnormal flow patterns resulting in thrombosis. However, the relationship of minor discontinuities to stent thrombosis or restenosis is less clear both in animals and in man.<sup>7</sup> In the current study, although we saw a fair number of strut discontinuities, they did not result in greater luminal compromise. It is likely that there is a tradeoff between early dismantling and strut discontinuities (Figure 6).

## Study Limitations

The present study has a number of limitations. First, the healthy porcine coronary model was used in this study, which is different from diseased human coronary arteries. The results were collected from different cohorts stratified by time, and therefore, the presence of vascular remodeling needs to be interpreted with caution. Also, the possibility of introducing additional injury and inflammation from consecutive imaging follow-up must be considered during conduction of preclinical long-term studies. ART-BRS was drug-free, which could be considered as currently not comparable to the current BRS. However, the properties of this platform have demonstrated its ability to result in early dismantling and late lumen enlargement despite lack of drug, and these have both been confirmed in human in the ARTDIVA trial. Besides, its safety (early complete re-endothelialization) could be of interest in large vessels for which neointimal suppression may not be mandatory. Finally, the ART-BRS platform is currently being used for the design of a drug-eluting stent.

## Conclusions

In this study, the ART-BRS exhibited a safety profile comparable to that of the control BMS up to 3 years; early significant luminal enlargement commenced at 3 months following implantation, which was associated with incremental inflammation for up to 6 months and a decrease thereafter. The early lumen enlargement distinguishes ART-BRS from other BRS made of PLLA, already in clinical use. Finally, the consecutive follow-up to 3 years of the current study confirmed the hypothesis that early dismantling of the ART-BRS is associated with continued lumen enlargement.

## Sources of Funding

The study was funded by Arterial Remodeling Technologies. CVPPath Institute Inc, a private no-profit research organization, provided partial support for this work.

## Disclosures

Dr Nakano has received speaking honoraria from Abbott Vascular, Boston Scientific, St Jude Medical, and Terumo Corporation. Dr Joner is a consultant for Biotronik and Cardionovum and has received speaking honoraria from Abbott Vascular, Biotronik, Medtronic, and St Jude. Dr Virmani receives research support from 480 Biomedical, Abbott Vascular, Atrium, Biosensors International, Biotronik, Boston Scientific, Cordis J&J, GSK, Kona, Medtronic, Microport Medical, OrbusNeich Medical, ReCore, SINO Medical Technology, Terumo Corporation, and W.L. Gore; Dr Lafont and Dr Vert are cofounders of ART, Mrs Mathieu is an employee of ART. Other authors have no conflict of interest to declare.

## References

1. Lafont A. Bioresorbable stents: the next horizon after drug eluting stents? *EuroIntervention*. 2007;3:21–23.
2. Onuma Y, Serruys PW. Bioresorbable scaffold: the advent of a new era in percutaneous coronary and peripheral revascularization? *Circulation*. 2011;123:779–797.
3. Ellis SG, Kereiakes DJ, Metzger DC, Caputo RP, Rizik DG, Teirstein PS, Litt MR, Kini A, Kabour A, Marx SO, Popma JJ, McGreevy R, Zhang Z, Simonton C, Stone GW. Everolimus-eluting bioresorbable scaffolds for coronary artery disease. *N Engl J Med*. 2015;373:1905–1915.
4. Serruys PW, Chevalier B, Sotomi Y, Cequier A, Carrie D, Piek JJ, Van Boven AJ, Dominici M, Dudek D, McClean D, Helqvist S, Haude M, Reith S, de Sousa Almeida M, Campo G, Iniguez A, Sabate M, Windecker S, Onuma Y. Comparison of an everolimus-eluting bioresorbable scaffold with an everolimus-eluting metallic stent for the treatment of coronary artery stenosis (ABSORB II): a 3 year, randomised, controlled, single-blind, multicentre clinical trial. *Lancet*. 2016;388:2479–2491.
5. Cassese S, Byrne RA, Ndrepepa G, Kufner S, Wiebe J, Repp J, Schunkert H, Fusaro M, Kimura T, Kastrati A. Everolimus-eluting bioresorbable vascular scaffolds versus everolimus-eluting metallic stents: a meta-analysis of randomised controlled trials. *Lancet*. 2016;387:537–544.
6. Garg S, Serruys PW. Coronary stents: looking forward. *J Am Coll Cardiol*. 2010;56:S43–S78.
7. Otsuka F, Pacheco E, Perkins LE, Lane JP, Wang Q, Kamberi M, Frie M, Wang J, Sakakura K, Yahagi K, Ladich E, Rapoza RJ, Kolodgie FD, Virmani R. Long-term safety of an everolimus-eluting bioresorbable vascular scaffold and the cobalt-chromium XIENCE V stent in a porcine coronary artery model. *Circ Cardiovasc Interv*. 2014;7:330–342.
8. Lafont A, Durand E. A.R.T.: concept of a bioresorbable stent without drug elution. *EuroIntervention*. 2009;5(suppl F):F83–F87.
9. Durand E, Sharkawi T, Leclerc G, Raveleau M, van der Leest M, Vert M, Lafont A. Head-to-head comparison of a drug-free early programmed dismantling polylactic acid bioresorbable scaffold and a metallic stent in the porcine coronary artery: six-month angiography and optical coherence tomographic follow-up study. *Circ Cardiovasc Interv*. 2014;7:70–79.
10. Nakatani S, Sotomi Y, Ishibashi Y, Grundeken MJ, Tateishi H, Tenekecioglu E, Zeng Y, Suwannasom P, Regar E, Radu MD, Raber L, Bezerra H, Costa MA, Fitzgerald P, Prati F, Costa RA, Dijkstra J, Kimura T, Kozuma K, Tanabe K, Akasaka T, Di Mario C, Serruys PW, Onuma Y. Comparative analysis method of permanent metallic stents (XIENCE) and bioresorbable poly-L-lactic (PLLA) scaffolds (Absorb) on optical coherence tomography at baseline and follow-up. *EuroIntervention*. 2016;12:1498–1509.



11. Onuma Y, Serruys PW, Perkins LE, Okamura T, Gonzalo N, Garcia-Garcia HM, Regar E, Kamberi M, Powers JC, Rapoza R, van Beusekom H, van der Giessen W, Virmani R. Intracoronary optical coherence tomography and histology at 1 month and 2, 3, and 4 years after implantation of everolimus-eluting bioresorbable vascular scaffolds in a porcine coronary artery model: an attempt to decipher the human optical coherence tomography images in the ABSORB trial. *Circulation*. 2010;122:2288–2300.
12. Finn AV, Kolodgie FD, Harnek J, Guerrero LJ, Acampado E, Tefera K, Skoricja K, Weber DK, Gold HK, Virmani R. Differential response of delayed healing and persistent inflammation at sites of overlapping sirolimus- or paclitaxel-eluting stents. *Circulation*. 2005;112:270–278.
13. Nakazawa G, Nakano M, Otsuka F, Wilcox JN, Melder R, Pruitt S, Kolodgie FD, Virmani R. Evaluation of polymer-based comparator drug-eluting stents using a rabbit model of iliac artery atherosclerosis. *Circ Cardiovasc Interv*. 2011;4:38–46.
14. Farooq V, Serruys PW, Heo JH, Gogas BD, Onuma Y, Perkins LE, Diletti R, Radu MD, Raber L, Bourantas CV, Zhang Y, van Remortel E, Pawar R, Rapoza RJ, Powers JC, van Beusekom HM, Garcia-Garcia HM, Virmani R. Intracoronary optical coherence tomography and histology of overlapping everolimus-eluting bioresorbable vascular scaffolds in a porcine coronary artery model: the potential implications for clinical practice. *JACC Cardiovasc Interv*. 2013;6:523–532.
15. Verheye S, Ormiston JA, Stewart J, Webster M, Sanidas E, Costa R, Costa JR Jr, Chamie D, Abizaid AS, Pinto I, Morrison L, Toyloy S, Bhat V, Yan J, Abizaid A. A next-generation bioresorbable coronary scaffold system: from bench to first clinical evaluation: 6- and 12-month clinical and multimodality imaging results. *JACC Cardiovasc Interv*. 2014;7:89–99.
16. Middleton JC, Tipton AJ. Synthetic biodegradable polymers as orthopedic devices. *Biomaterials*. 2000;21:2335–2346.
17. Vert M. Aliphatic polyesters: great degradable polymers that cannot do everything. *Biomacromolecules*. 2005;6:538–546.
18. Lafont A, Mensah-Gourmel J. Bioresorbable coronary scaffolds should disappear faster. *Lancet*. 2016;387:1275–1276.
19. Puricel S, Cuculi F, Weissner M, Schmermund A, Jamshidi P, Nyffenegger T, Binder H, Eggebrecht H, Munzel T, Cook S, Gori T. Bioresorbable coronary scaffold thrombosis: multicenter comprehensive analysis of clinical presentation, mechanisms, and predictors. *J Am Coll Cardiol*. 2016;67:921–931.
20. Moriyama N, Shishido K, Tobita K, Takada T, Ochiai T, Tsukuda S, Yamanaka F, Sugitatsu K, Mizuno S, Tanaka Y, Murakami M, Matsumi J, Takahashi S, Akasaka T, Saito S. Persistent bioresorbable vascular scaffold by optical coherence tomography imaging at 5 years. *JACC Cardiovasc Interv*. 2017;10:e11–e13.
21. Foin N, Lee R, Mattesini A, Caiazzo G, Fabris E, Kilic D, Chan JN, Huang Y, Venkatraman SS, Di Mario C, Wong P, Nef H. Bioabsorbable vascular scaffold overexpansion: insights from in vitro post-expansion experiments. *EuroIntervention*. 2016;11:1389–1399.
22. Karanasos A, Van Mieghem N, van Ditzhuijzen N, Felix C, Daemen J, Autar A, Onuma Y, Kurata M, Diletti R, Valgimigli M, Kauer F, van Beusekom H, de Jaegere P, Zijlstra F, van Geuns RJ, Regar E. Angiographic and optical coherence tomography insights into bioresorbable scaffold thrombosis: single-center experience. *Circ Cardiovasc Interv*. 2015;8:e002369. DOI: 10.1161/CIRCINTERVENTIONS.114.002369.
23. Onuma Y, Serruys PW, Muramatsu T, Nakatani S, van Geuns RJ, de Bruyne B, Dudek D, Christiansen E, Smits PC, Chevalier B, McClean D, Koolen J, Windecker S, Whitbourn R, Meredith I, Garcia-Garcia HM, Veldhof S, Rapoza R, Ormiston JA. Incidence and imaging outcomes of acute scaffold disruption and late structural discontinuity after implantation of the ABSORB everolimus-eluting fully bioresorbable vascular scaffold: optical coherence tomography assessment in the ABSORB cohort B trial (a clinical evaluation of the bioabsorbable everolimus eluting coronary stent system in the treatment of patients with de novo native coronary artery lesions). *JACC Cardiovasc Interv*. 2014;7:1400–1411.